Experimental Mechanics (2006) 46: 531–542
DOI 10.1007/s11340-006-8351-y

Phase-Transformation Fronts Evolution for Stress- and Strain-Controlled Tension Tests in TiNi Shape Memory Alloy

E.A. Pieczyska · S.P. Gadaj · W.K. Nowacki · H. Tobushi

Received: 13 October 2005 / Accepted: 17 March 2006 / Published online: 16 May 2006

Abstract Nucleation and development of phase transformation fronts in TiNi shape memory alloy subjected to the stress- and strain-controlled tension tests were investigated. A thermovision camera was applied to register the distribution of infrared radiation emitted by the specimen and to find its temperature variations. During the loading, narrow bands of considerably higher temperature corresponding to the martensitic phase, starting from the central part of the specimen and developing towards the specimen grips, under both approaches, were registered. The inclined bands of heterogeneous temperature distribution were observed also during the unloading process of the SMA, while the reverse transformation accompanied by temperature decrease took place. Thermomechanical aspects of martensitic and reverse transformations for various strain rates were analyzed under both stress- and strain-controlled tests.

Keywords Shape memory alloy · Martensitic transformation · Phase transformation front · Temperature change · Stress-controlled test · Strain-controlled test · Infrared thermography

E.A. Pieczyska (✉) · S.P. Gadaj · W.K Nowacki
Institute of Fundamental Technological Research,
Polish Academy of Sciences, Świętokrzyska 21,
00-049 Warsaw, Poland
e-mail: epiecz@ippt.gov.pl

H. Tobushi (SEM member)
Department of Mechanical Engineering,
AICHI Inst. of Technology, 1247, Yachigusa, Yakusa-cho,
Toyota, Aichi 470-0392, Japan
e-mail: tobushi@aitech.ac.jp

Introduction

New functions and wide capabilities are expected by multifunctional intelligent materials, possessing various functions in differing environmental conditions [1, 2]. Among the various kinds of intelligent materials, shape memory alloys (SMAs) characterized by a complex combination of functions, like sensing, processing and actuating functions, based on shape memory effect and superelasticity, are expected to be widely applied in the near future [3]. Most widely used in practical applications are TiNi SMAs which are characterized by their excellent shape memory properties, sufficient strengths and ductility, high corrosion resistance and good biocompatibility. These characteristics enable SMAs to find applications in car, aircraft and fine machine industries, daily equipment and medicine [3–12].

Under uniaxial loading of the TiNi SMA, the phase transitions are often accompanied by unstable mechanical behavior and localized transformation, resulting in propagating transformation fronts. They are characterized by significant non-uniform deformation and temperature fields. These phenomena have been studied experimentally in detail in [13, 14] and the effects were confirmed in [15–17]. The interesting results of the localized phase transformation obtained for microtubes were presented in [18, 19] and completed with a proposed model in [20]. Two almost perpendicular directions of the transformation bands, developing towards the specimen grips, were observed using an infrared camera in [21–24]. The transformation-induced stress relaxation effects were discussed in [23, 24]. Recoverable energy and dissipated strain energy were evaluated under both temperature-controlled and -uncontrolled conditions for various strain rates in [25]. An interesting model on the localized nucleation and

propagation phenomena for the wide range of loading rates and ambient thermal conditions was presented in [26]. Measurement of inhomogeneous deformation behavior arising in SMA was described in [27]. The thermal and calorimetric effects induced by Lüders bands propagation in steel, related also to SMA, were analyzed in [28]. The conditions under which the Lüders-like deformation in SMA can be observed, as well as can be eliminated, are specified in details in [29]. However, based on the results presented in this paper, it is difficult to agree with all of the above [29].

The objective of the work is the thermomechanical aspect of the stress-induced phase transformations in TiNi SMA, namely an investigation into the onset and growth of the martensitic and the reverse transformation fronts on the basis of contact-less specimen temperature variations. Depending on the applications, the SMA elements may be controlled by force or by displacement and so the study comprises both the stress- and strain-controlled conditions. The subloop deformation behavior with cyclic loading, transformation-induced creep and stress relaxation depend on strain rate and stress rate [30]. Since the applied behaviors of SMAs are strongly temperature dependent, a study of their thermomechanical properties is of key value.

The investigations into measurements of the temperature accompanying the deformation process of SMAs have been launched quite recently [6–17]. At first the temperature was estimated using a thermocouple, which, however, limited the measurement to only a single chosen point [6]. Application of an infrared technique allows monitoring of the temperature distribution on the examined specimen surface, measurement of a mean temperature over a chosen area, an arbitrarily chosen segment or chosen points [13–17, 21–26, 28].

In the present paper, nucleation and development of the martensite and reverse transformations fronts in TiNi SMA subjected to various stress- and strain-controlled tension tests using a smart thermovision camera were investigated.

Experimental Procedure

The tension tests were carried out on a belt type specimen of 160 × 10 × 0.4 mm, cut off from a strip of TiNi SMA of the constitution Ti-55.3wt.% Ni and characterized by the austenite finish temperature A_f equal to 283 K. Since the A_f temperature is so low, the TiNi SMA demonstrates a complete loop of pseudo-elasticity during the tests carried out at room temperature. Before the testing, the specimen surface was covered with a very thin layer of carbon black powder in order to make its emissivity higher and more homogeneous. All investigations were performed at room temperature of about 296 K. The specimens were subjected to a strain-controlled tension test with various strain rate and stress-controlled tension tests with various stress rate in the quasi-static range of deformation. In the course of investigations both the mechanical characteristics and the distribution of the infrared radiation emitted by the specimen surface were continuously registered. The stress and the strain quantities were related to the current (instantaneous) value of the specimen cross-section and thickness values. The temperature distribution was registered by using infrared equipment allowing for infrared photographs, i.e., thermograms, to be stored in digital form with a maximal frequency of 50 Hz. That allows reproduction of the images at any moment and makes the calculation of temperature as well as its presentation straightforward. This can be presented as a function of time or other parameters of the deformation process.

The infrared camera used is long wave type, working in the wave range of 7.5–13 μm. The matrices size is 320 × 240 pixels. The spatial and the temperature resolutions depend on the camera-specimen distance. In the case of the measurement presented in the paper, the distance was 10 cm and the spatial resolution was 0.3 mm. The measurement temperature sensitivity, in the range up to 30 K, is below 0.08 K.

For these investigations three kinds of temperature registration were applied:

- temperature distribution on the specimen surface,
- mean temperature taken from the chosen specimen area,
- change in temperature of a chosen point on the specimen surface.

The temperature distribution on the specimen surface immediately reflects the origin and development of the new phases, both martensite and reverse, due to the significant temperature variations between the parent and the new phase.

The average temperature was calculated over an area of 8 × 60 mm, located in the central part of the specimen. It was used in the thermomechanical coupling analysis.

The point temperature was taken from the part of the specimen surface where the first band of the higher temperature related to the new, martensite phase was noticed.

The temperature and mechanical data enable the analysis of the nucleation process and further development of both the martensitic and the reverse transformations.

Superelastic Behavior of TiNi SMA During Stress- and Strain-Controlled Tension Tests with Various Strain Rates

The stress–strain curves for the strain rates of 5×10^{-4} s^{-1}; 5×10^{-3} s^{-1}, 5×10^{-2} s^{-1} and 10^{-1} s^{-1} under strain-controlled conditions are shown in Fig. 1(a), and the curves obtained under stress-controlled conditions with the stress rates of 12.5, 25, 50 and 75 MPa s^{-1} are shown in Fig. 1(b).

For all stress and strain rates, the pseudoelasticity effects were registered for both approaches. After an elastic deformation the martensitic transformation starts. Its initial homogeneous stage, accompanied by uniform, small temperature increase, is followed by the waving part of the stress–strain curves, manifested by shear-like bands with significant temperature rise, similar to that observed in Lüders inhomogeneous deformation [13–29]. Next, the upswing region is observed, manifested by a more advanced and more homogeneous stage of the phase transformation, accompanied by the more uniform temperature distribution, (see next chapters).

During the process of unloading, after passing its elastic stage, the reverse transition initiates. After it is completed, the material almost returns to the parent austenite phase. However, the residual strains, related to a small amount of the residual martensite and irreversible macro-structural changes appear, depending on the specimen history.

Influence of Strain Rate on Mechanical and Temperature Characteristics

The investigations conducted have proved that the run of the stress–strain curves depends on the strain rate applied under both approaches. However, the influence of the strain rate is stronger for the strain-controlled tests. During phase transformation, stress magnitudes increase as the strain rate grows, since the temperature increases while the deformation process develops [8, 9, 11–17]. The stress–strain curve developing at a very low strain rate of 10^{-4} s^{-1} is almost flat, like the typical curve illustrating the phenomenon of pseudo-elasticity in SMAs, found for low strain rates [6, 11]. For higher strain rates, the slope of inclination of the segments of stress–strain curves, corresponding to the martensitic and the reverse transformations is steeper. The higher the strain rate, the steeper the slope of the curve.

Temperature changes vs. stress for TiNi SMA obtained by the tension tests with various stress and strain rates under the stress- and strain-controlled conditions are presented in Fig. 2(a) and (b), respectively.

One can observe that the higher the strain rate the higher the temperature change for both the stress- and strain-controlled tests. After the initial homogeneous range of deformation, a significant temperature in-

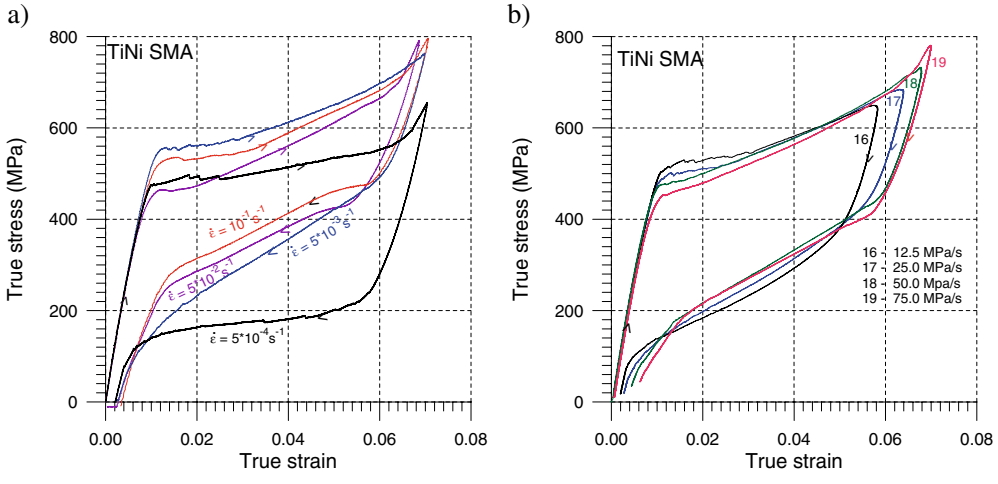

Fig. 1. Stress-strain curves of TiNi SMA subjected to (**a**) strain-controlled tension tests with strain rates: 5×10^{-4} s^{-1}; 5×10^{-3} s^{-1}, 5×10^{-2} s^{-1}, 10^{-1} s^{-1}, and (**b**) stress-controlled tension tests with stress rates: 12.5, 25, 50, 75 MPa s^{-1}. (E. A. Pieczyska, S. P. Gadaj, W. K. Nowacki and H. Tobushi)

crease, related to the exothermic martensitic transformation, is observed. The highest temperature increase is observed at the end of the martensitic transformation and it changes from 26 to 40 K, depending on the strain rate applied (Fig. 2). When unloading, the temperature drops as the stress decreases. First, at the elastic unloading, a slow temperature decrease can be observed, caused by heat exchange with the surroundings. Then, the temperature drops rapidly due to the endothermic reverse transformation. One can notice that the segments of the curves related to the martensite and the reverse phase transformations are almost parallel to each other, irrespective of the strain rate or stress rate applied. After the reverse transformation is completed, the temperature drops below the room temperature. The lowest temperature drop of 9 K was found for the stress-controlled test with the lowest stress rate of 12.5 MPa/s, caused by heat transfer and stronger grip influence under these conditions.

Theoretical Background and Conditions for Progress of Martensitic and Reverse Phase Transformations

According to the constitutive relationships proposed by Tanaka [4] and Tanaka et al. [5, 6], and applied by Tobushi et al. [10] and Lin et al. [11], the deformation behavior of SMA due to martensitic transformation can be described as follows Fig. 3(a):

$$\dot{\sigma} = D\dot{\varepsilon} + \theta\dot{T} + \Omega\dot{\xi}; \tag{1}$$

where σ, ε and T represent the stress, strain and temperature, respectively. The coefficients D and θ represent the modulus of elasticity and the thermoelastic constant, respectively. The quantity (Ω/D) represents the strain range of the martensitic transformation. The internal state variable ξ represents the volume fraction of the martensite phase. In this way, the volume fraction of the parent phase is $1-\xi$. The dot over the symbols denotes the time derivative. The transformation kinetics for the martensitic transformation can be described by the formula:

$$\frac{\dot{\xi}}{1-\xi} = b_M C_M \dot{T} - b_M \dot{\sigma} \geq 0 \tag{2}$$

and for the reverse transformation:

$$-\frac{\dot{\xi}}{\xi} = b_A C_A \dot{T} - b_A \dot{\sigma} \geq 0 \tag{3}$$

The material parameters: b_M, C_M, b_A and C_A are determined from the experiment, carried out at various temperatures. Assuming the parameters constant:

$$\dot{\xi} = 1 - \exp\{b_M C_M (M_s - T) + b_M \sigma\} \tag{4}$$

$$\dot{\xi} = \exp\{b_A C_A (A_s - T) + b_A \sigma\}, \tag{5}$$

where M_s and A_s stand for the temperatures at which the martensite transformation and the reverse transformation start under the stress-free conditions, respectively.

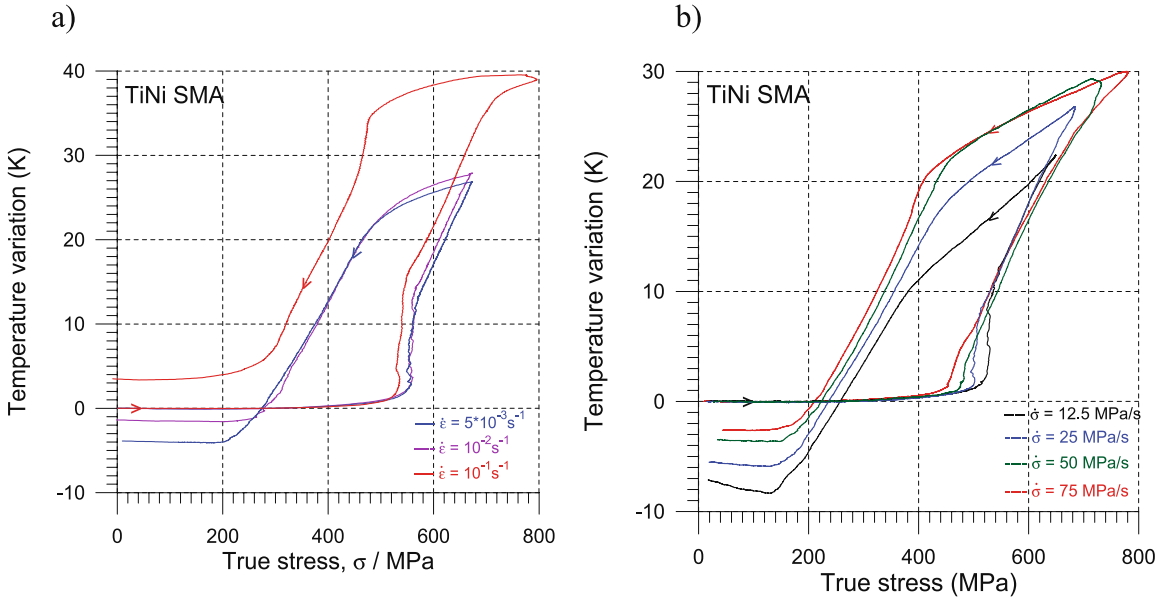

Fig. 2. Temperature changes vs. stress in TiNi SMA subjected to (**a**) strain-controlled tension test with strain rates 5×10^{-3} s^{-1}, 10^{-2} s^{-1}, 10^{-1} s^{-1}, and (**b**) stress-controlled tension test with stress rates 12.5, 25, 50, 75 MPa s^{-1}. (E. A. Pieczyska, S. P. Gadaj, W. K. Nowacki and H. Tobushi)

The starting and completing lines for the martensite transformation can be expressed by the straight lines with a slope of C_M:

$$\sigma = C_M(T - M_s) \tag{6}$$

$$\sigma = C_M(T - M_s) - 2\ln 10/b_M \tag{7}$$

The starting and completing lines for the austenite transformation can be expressed by the straight lines with a slope of C_A:

$$\sigma = C_A(T - A_S) \tag{8}$$

$$\sigma = C_A(T - A_S) - 2\ln 10/b_A \tag{9}$$

The transformation regions prescribed by the transformation lines, according to the equations (6), (7), (8), (9) are shown in Fig. 3(a).

The conditions for the progress of the martensitic transformation, [equation (2)] become:

$$b_M C_M \dot{T} \geq b_M \dot{\sigma} \quad b_M < 0; \text{ therefore :} \tag{10}$$

$$\frac{d\sigma}{dT} \geq C_M \quad \text{for } dT > 0, \text{ and } \frac{d\sigma}{dT} \leq C_M \quad \text{for } dT < 0 \tag{11}$$

The conditions for the progress of the reverse transformation, (equation 3) become:

$$b_A C_A \dot{T} \geq b_A \dot{\sigma} \quad b_A > 0; \text{ therefore :} \tag{12}$$

$$\frac{d\sigma}{dT} \leq C_A \qquad \text{for } dT > 0 \text{ and } \frac{d\sigma}{dT} C_A \text{ for } dT < 0 \tag{13}$$

Based on the tests carried out with various strain rates and, related to this, various temperature increments shown in Fig. 2, the stress-temperature graphs in Fig. 3(b) are proposed to estimate the general conditions for the progress of the martensitic and reverse transformations during the stress-induced phase transformation at room temperature. The conditions for the start and finish of the martensitic transformation are expressed by the transformation lines M_s (Martensite start) and M_f (Martensite finish), while the conditions for the start and finish of the reverse transition are expressed by the lines A_s (Austenite start) and A_f (Austenite finish), respectively. The transformation progresses in the strip areas between the start and finish lines, respectively.

The M_s, M_f, A_s and A_f lines are necessary to be determined based on the data under low strain rate, i.e., under the quasi-static isothermal conditions. This condition can be obtained under the strain rate below 1.7×10^{-4} s^{-1}. In the case of a higher strain rate, not only stress but also temperature increases due to the martensitic phase transformation and decreases due to the reverse transformation. If we take into account the variation in temperature due to the martensitic transformation, these lines and the deformation behavior of the material can be evaluated. That is, if the stress-temperature data for different strain rates are plotted on the same chart while considering the variation in temperature, these lines are located parallel to each other, that is, the slopes of the lines take the same values [Fig. 2(a), (b)]. The conditions for the start and finish of the martensitic and reverse transitions presented in Fig. 3(b), expressed by the lines M_s and M_f and by the lines A_s and A_f, respectively, are only an estimation. However, their run is in agreement to the obtained data for the tests performed at various stress and strain rates, according to the Clausius–Clapeyron formula.

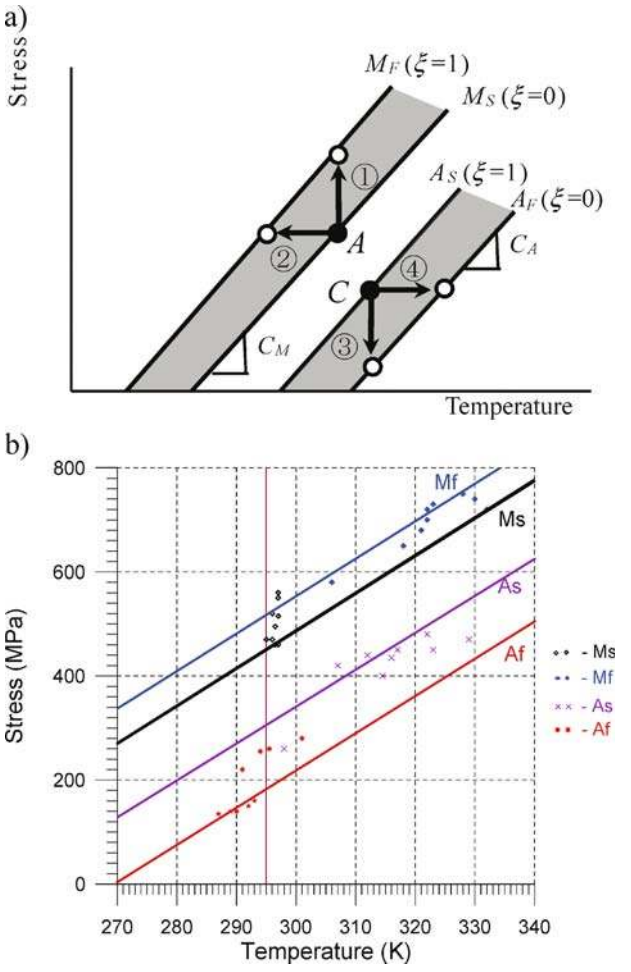

Fig. 3. (**a**) Conditions for progress of martensitic and reverse transformations. (**b**) Estimated paths for progress of martensitic and reverse transformation in TiNi SMA under stress- and strain-controlled tension tests with various stress and strain rates; M_s Martensite start, M_f martensite finish, A_s austenite start, A_f austenite finish. (E. A. Pieczyska, S. P. Gadaj, W. K. Nowacki and H. Tobushi)

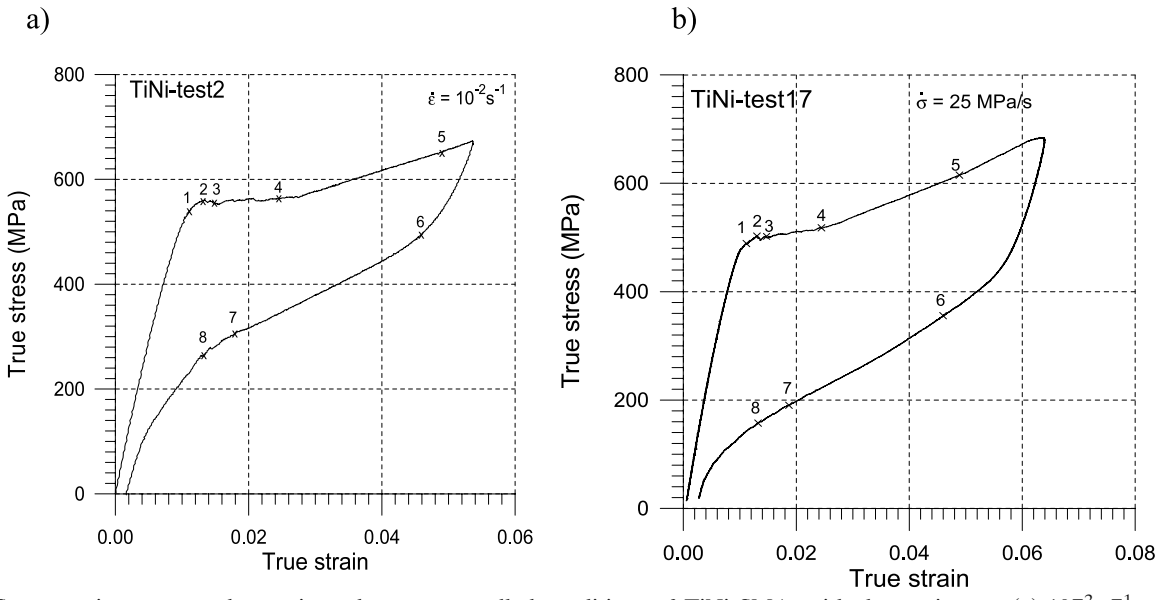

Fig. 4. Stress-strain curves under strain and stress controlled conditions of TiNi SMA, with the strain rate (**a**) 10^{-2} s^{-1} and stress rate (**b**) 25 MPa s^{-1}. (E. A. Pieczyska, S. P. Gadaj, W. K. Nowacki and H. Tobushi)

Onset and Development of Phase Transformation Fronts

Two tests were chosen, with the strain rate of 10^{-2} s^{-1} [Fig. 4(a)], and the stress rate of 25 MPa s^{-1} [Fig. 4(b)], in order to analyze the onset and growth of the stress-induced phase transformation fronts and to discuss the similarities and the discrepancies between the stress- and strain-controlled approaches. The temperature distributions for the tests are shown in thermograms in Fig. 6: the left side for the strain-controlled test and the right side, for the stress-controlled test, respectively. One can see that the points corresponding to the thermograms shown in Fig. 6 are marked on the stress–strain curves (Fig. 4) and the numbers over thermograms correspond to the points marked on Fig. 4(a), (b). The chosen thermograms are very characteristic of the phenomena occurring during the martensitic and the reverse transformations. The graphs, shown in Fig. 5(a) prove why such stress- and strain-controlled tests were taken into consideration. Namely, the rate of deformation, which seems to be mainly responsible for the transformation conditions, is similar for just these two chosen tests [Fig. 5(a)]. The segment of curve for the stress-controlled test, related to the martensitic transformation, is parallel to the segment of the strain-controlled curve. However,

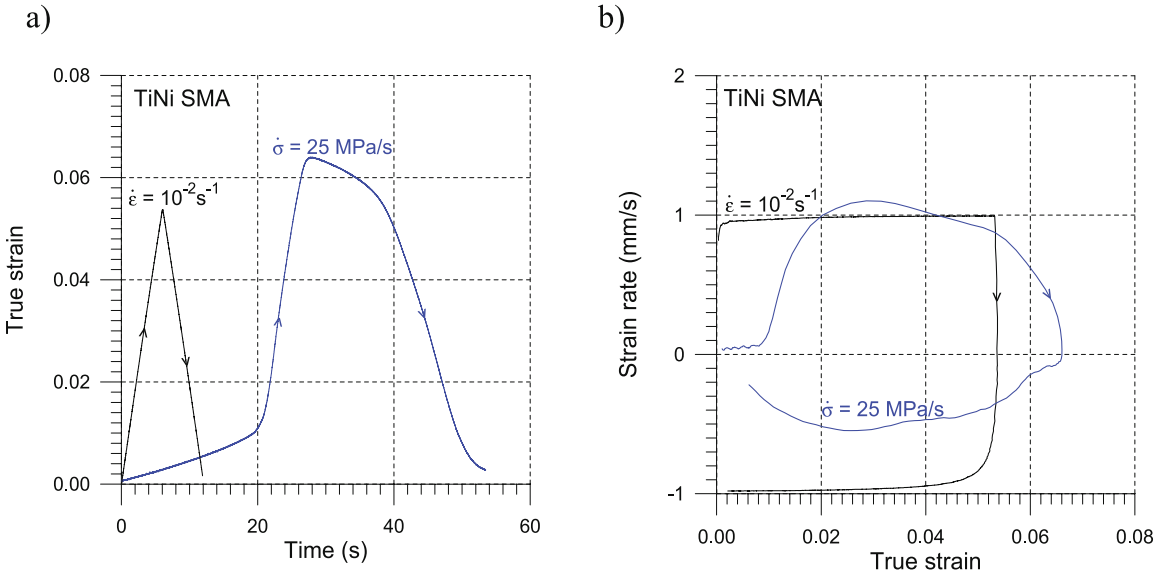

Fig. 5. Comparison of (**a**) strain vs. time and (**b**) strain rate vs. strain for progress of martensite and reverse transformations under strain and stress controlled tests. (E. A. Pieczyska, S. P. Gadaj, W. K. Nowacki and H. Tobushi)

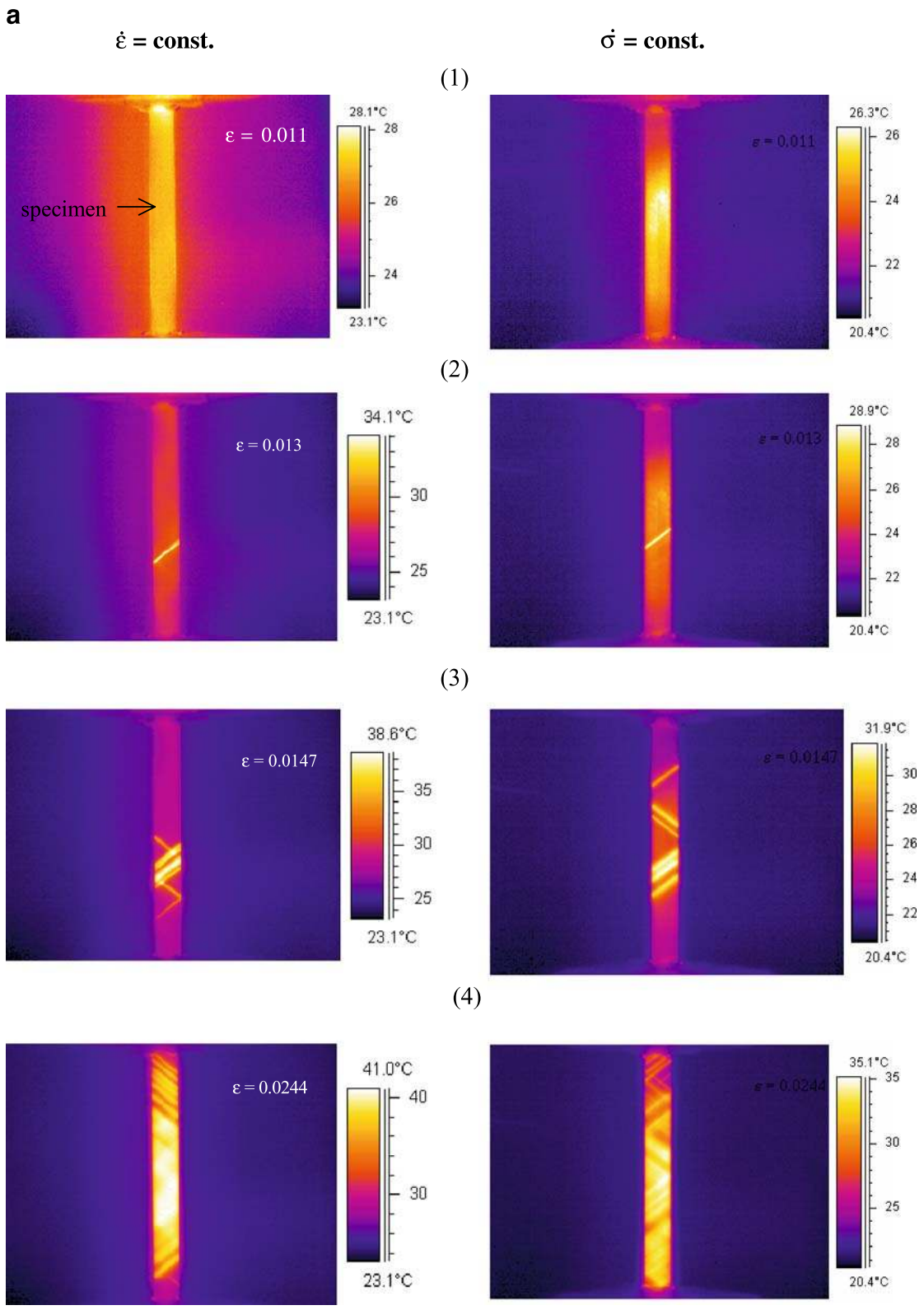

Fig. 6. Temperature distribution of TiNi SMA subjected to tension test at room temperature with constant strain rate 10^{-2} s^{-1} (*left side*) and constant stress rate 25 MPa/s (*right side*); numbers of thermograms correspond to points at the curves in Fig. 4: 1,2,3,4,5 loading; 6,7,8 unloading. (E. A. Pieczyska, S. P. Gadaj, W. K. Nowacki and H. Tobushi)

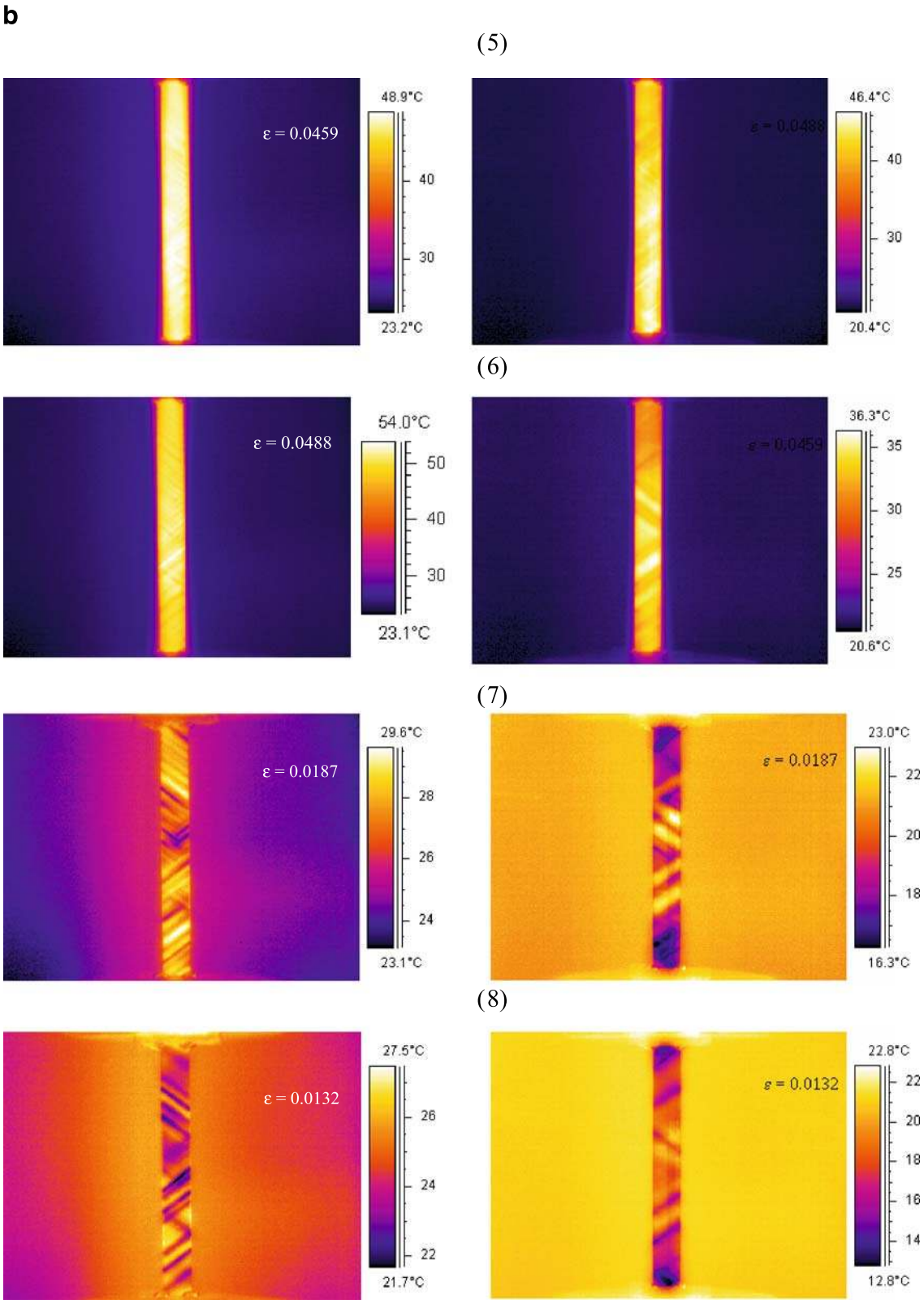

Fig. 6. continued

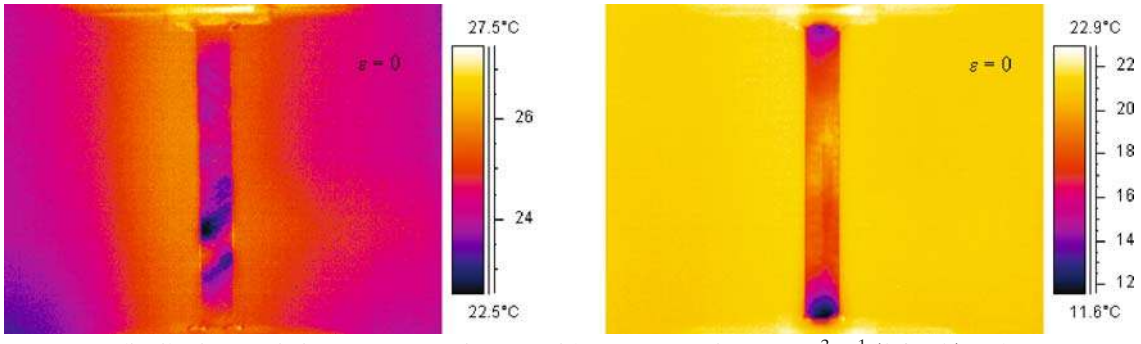

Fig. 7. Temperature distribution of TiNi SMA after tension test with constant strain rate 10^{-2} s^{-1} (*left side*) and constant stress rate 25 MPa/s (*right side*): σ, ε = 0. (E. A. Pieczyska, S. P. Gadaj, W. K. Nowacki and H. Tobushi)

during the reverse transformation the conformity is not so good. The calculated discrepancies in the strain rates are shown in Fig. 5(b). The strain range chosen for two tests is also not equal. Nevertheless, just these tests were taken into account due to the mechanical data being similar and the thermograms of the phase-transitions phenomena turning out to be of best quality.

The uniform temperature distribution on the specimen surface indicates the homogeneity of the stress and the strain state along the specimen. Before tension started, the temperature of the specimen was uniform and equal to the ambient temperature of 296 K. At the initial tension stage, i.e., as the stress increases to its local maximum [see Fig. 4(a) and (b)], the temperature of the specimens surface grows. The thermal image, however, remains almost uniform indicating the homogeneous nature of the phase transformation process at this initial stage under both approaches [see Figs. 4, 6(1)]. During loading, the temperature distribution became non-homogeneous; the increase of temperature in some areas of the specimen was higher than in others (Fig. 6).

When the true strain value reached 0.013, a line of higher temperature evolving into a narrow band appeared on the specimen surface proving the initiation of the localized martensite transformation [Fig. 6(2)]. The band made an angle of 48° with the direction of tension. The temperature difference in the area where the band appears is about 8 K, proving the rapid nature of the process. As the tension proceeds the band significantly widens and other bands appear at first parallel and then inclined at the same angle but in the opposite direction [Fig. 6(3)]. The highest temperature was registered at the intersection of the bands. However, the mean temperature of the specimen surface also increased during the process.

At higher strain level, more and more lines evolving into bands appear finally reaching the specimen grip [Figs. 4, 6(4)]. Due to heat flow and the more advanced process, the thermal image becomes more ambiguous. At this stage of deformation, the wavy part of the stress–strain curves, related to the onset and movement of the bands, ends and is followed by the upswing region of the curve. At the final phase of tension, the increase in temperature exceeds 27 K for this strain rate (Fig. 2).

In the course of unloading, bands of significantly lower temperature appear. They are, however, rather uniformly distributed on the specimen surface, proving that the reverse transformation also develops in an inhomogeneous way [Fig. 6(6, 7, 8)]. The temperature of the specimen at the end of unloading is lower than

Table 1

	Martensitic Transformation		Reverse Transformation	
	Δσ	Δ*T*	Δσ	Δ*T*
$\dot{\varepsilon} = const$	+200 MPa	+36 K	−190 MPa	−28 K
$\dot{\sigma} = const$	+270 MPa	+26.5 K	−240 MPa	−21.5 K

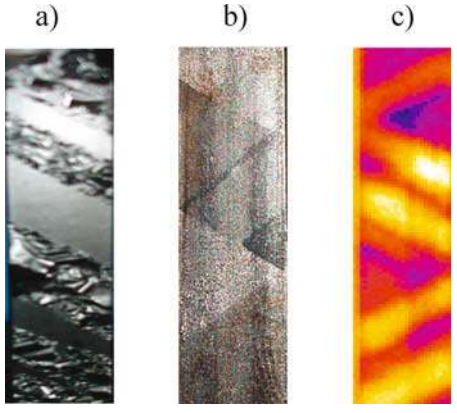

Fig. 8. Localized phase transformation bands in TiNi SMA observed in various techniques: (**a**) optical photograph of trace of the transformation bands on the specimen surface covered by spray with black lacquer, (**b**) optical photograph of relief of the transformation bands on the specimen surface covered by black marking ink, (**c**) infrared image of the transformation band. (E. A. Pieczyska, S. P. Gadaj, W. K. Nowacki and H. Tobushi)

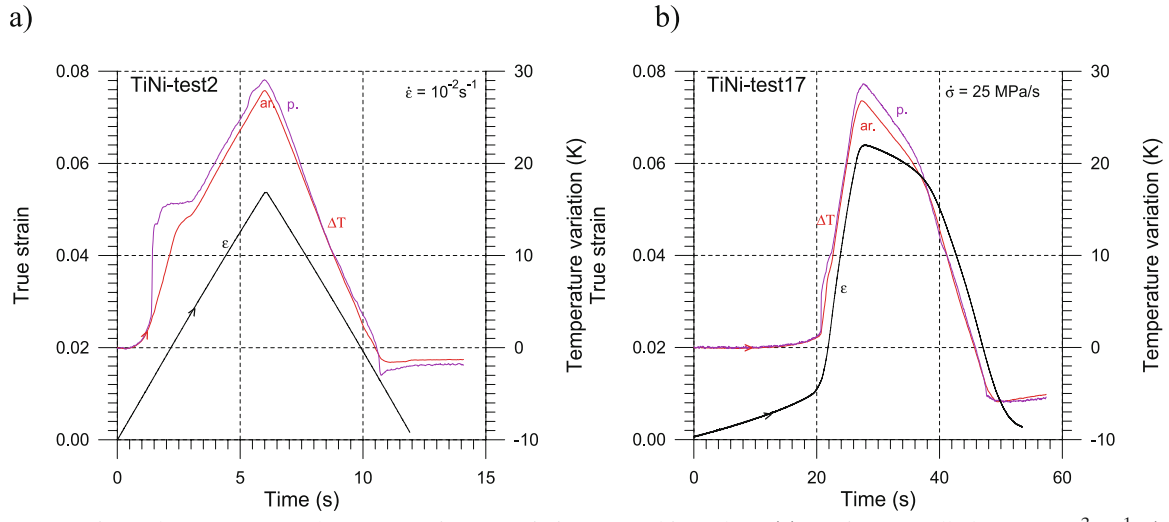

Fig. 9. True strain and temperature changes vs. time of TiNi SMA subjected to (**a**) strain controlled test—10^{-2} s^{-1}; (**b**) stress controlled test—25 MPa/s ; ΔT Average temperature change from the specimen surface, ΔT_P temperature change in the point where the martensite transformation start was noticed. (E. A. Pieczyska, S. P. Gadaj, W. K. Nowacki and H. Tobushi)

the initial temperature of the specimen, before testing [Figs. 2, 6(8)].

After the unloading is completed, the temperature distribution still remained heterogeneous (Fig. 7) which could be explained in the following way. After unloading, some residual martensite remained. That is, though the reverse transformation was completed macroscopically, it was not completed microscopically. Based on this residual martensite, residual or internal stress after unloading might appear. Therefore, some local microscopic reverse transformation still occurs after the macroscopic completion of the reverse transition. Due to this effect, heterogeneous temperature distribution may appear after unloading. This point will be studied in more details during future research on the cyclic tests performed on the same TiNi SMA.

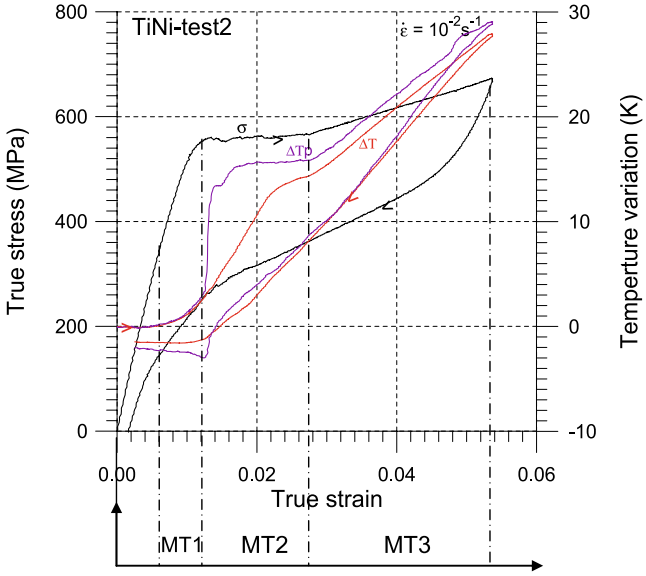

Fig. 10. Three stages of phase transformations: M1, M2 and M3 distinguished on the stress and temperature vs. strain curves for TiNi SMA subjected to tension test with the strain rate of 10^{-2} s^{-1}: ΔT Average temperature change in the testing area, ΔT_P temperature change at the point where the phase transition start was noticed. (E. A. Pieczyska, S. P. Gadaj, W. K. Nowacki and H. Tobushi)

Discussion

The phase transformation processes are strongly temperature dependent. In the deformations occurring within the range of quasi-static strain rates, some heat is released during the martensitic transformation that involves an increase in the specimen temperature. The changes in the material temperature, in turn, affect a stress increase in the specimen during the martensitic transformation. The influence also appears on the behavior of the $\sigma(\varepsilon)$ curves (Fig. 1). Similar phenomena, however in the opposite direction, can be observed during the unloading process, when the reverse transformation takes place. As a result both the stress level and the shape of stress–strain curves depend crucially on the strain rate applied and, related to this, the specimen temperature. The run of the curves depends on the temperature conditions, according to the SMA A_f temperature, as well as on the current temperature of the specimen, caused both by heat production and heat transfer. In this way, the presented curves differ from those obtained under the temperature-controlled conditions [10], i.e., the stress

level is higher for the higher strain rates and significantly steeper [21, 22]. Therefore, energy dissipation related to the phase transformations also changes depending on the strain rate and the test conditions. This was discussed in [25]. The estimated values in the stress $\Delta\sigma$ and the temperature ΔT variations due to the inhomogeneous martensitic and the reverse transformations taken for the maximal stress rate and the strain rate applied for the strain- and stress-controlled tests are shown in Table 1. The data were taken from the temperature vs. stress curves presented in Fig. 2(a) and (b), respectively.

It can be concluded on the grounds of the obtained results that no significant difference was observed between stress- and the strain-controlled conditions, according to the transformation bands onset and development. For all the strain rates applied in both approaches the martensitic and the reverse transformations in TiNi SMA are inhomogeneous processes. The narrow inclined Lüders-like bands of the martensitic phase are observed starting from the central part of the specimen and developing towards the specimen grips. They are characterized by a temperature increase of 8 K and inclination towards the tension direction of 48°. The phenomenon is so strong that the bands can also be observed directly by the naked eye on the specimen surface covered by lacquer or marking ink (Fig. 8).

During the stress-controlled tests, almost immediately and at several points on the specimen surface, the bands related to the new phase appear and they are wider. Temperature distributions are more uniform and the changes are smoother [Fig. 2(b), Fig. 6 right side].

This is also confirmed by the average and the point temperature changes [Fig. 9(a) and (b)] when the discrepancies between the temperature variations at the point and the average temperature are smaller in the stress-controlled conditions. So the whole process of the martensitic and the reverse transformation seems to be more homogeneous.

Based on mechanical and temperature characteristics, the three stages of the phase transformation can be distinguished during the TiNi SMA loading (Fig. 10): M1 homogeneous, characterized by uniform small temperature increase, M2 heterogeneous, manifested by Lüders-like bands of higher temperature, and finally M3 almost homogeneous again, related to the significant but more uniform temperature increase. The reverse transition occurs also in an inhomogeneous way, which was confirmed by the non-uniform temperature distributions registered during unloading of the TiNi SMA under both the stress- and strain-controlled conditions.

Conclusions

During the stress-induced phase transformations in TiNi SMA subjected to the temperature-uncontrolled tests, stress increases as the strain rate grows under both the stress- and strain-controlled conditions.

For both the approaches, the thermomechanical behavior of the SMA confirms the exothermic character of the austenite into martensite transformation and the endothermic character of the reverse transformation. The average temperature changes are up to 40 K for the highest strain rate applied.

Based on mechanical and temperature characteristics, the three stages of the phase transformation can be distinguished during the TiNi SMA loading: the homogeneous stage, characterized by a uniform, small temperature increase, the second heterogeneous stage, manifested by the Lüders-like bands of higher temperature, and the finally almost homogeneous stage, related to significant but more uniform temperature distribution. The reverse transitions also occurs in the inhomogeneous way, which was confirmed by the non-uniform temperature distributions registered during unloading of the TiNi SMA under both the stress- and strain-controlled conditions.

For both the approaches, the narrow bands of significantly higher temperature, related to the nucleation of the martensitic phase, or lower temperature, related to the reverse one, similar to the Lüders bands, were observed to start from the central part of the specimen and to develop towards the specimen grips.

The bands of the new phase, characterized by the angle of inclination with the direction of tension 48° and the variation in temperature of about 8 K, were followed by the next generation of the bands inclined at the same angle but in the opposite direction.

The more advanced phase transformation is related to the upswing region of the stress vs. strain curve, when the martensitic transformation was more homogeneous and both the mechanical as well the temperature curves were almost smooth.

Some discrepancies observed between the stress- and the strain-controlled tests were caused by the various instantaneous strain rates and related to the different heat transfer conditions and stronger grip influence.

Acknowledgments This research has been carried out with the support of Polish Grant No. 4T08A06024, the JSPS Grants: No.13650104(C), Post-doc PO4774, Joint Research supported by JSPS and PAS: No. 6612. The authors also would like to thank Prof. B. Raniecki (IFTR) and Prof. S. Miyazaki (Tsukuba Univ.) for fruitful discussions, as well as to extend their gratitude to L. Urbanski (IFTR), K. Hoshio and other students of AIT Japan, for technical advice.

References

1. Otsuka K, Wayman CM (1998) (eds) Shape memory materials. Cambridge University Press, Cambridge.
2. Funakubo H (1998) (ed) Shape memory alloys. Gordon and Breach, New York.
3. Duering TW, Melton KN, Stockel D, Wayman CM (1990) (eds) Engineering aspects of shape memory alloys. Butterworth-Heinemann, London.
4. Tanaka K (1986) A thermomechanical sketch of shape memory effect: one-dimensional tensile behavior. Res Mech 18:251–263.
5. Tanaka K, Kobayashi S, Sato Y (1986) Thermomechanics of transformation pseudoelasticity and shape memory effect in alloys. Int J Plast 2:59–72.
6. Tanaka K, Nishimura F, Tobushi H (1995) Transformation start lines in TiNi and Fe-based shape memory alloys after incomplete transformation induced by mechanical and/or thermal loads. Mech Mater 19:271–280.
7. Lin PH, Tobushi H, Ikai A, Tanaka K (1995) Deformation properties associated with the martensitic and R-phase transformations in TiNi shape memory alloy. J Appl Biomech 10(2):1–11.
8. Tobushi H, Shimeno Y, Hachisuka T, Tanaka K (1998) Influence of strain rate on superelastic properties of TiNi shape memory alloy. Mech Mater 30:141–150.
9. Tobushi H, Takata K, Shimeno Y, Nowacki WK, Gadaj SP (1999) Influence of strain rate on superelastic behavior of TiNi shape memory alloy. Proc Inst Mech Eng 213, Part L:93–102.
10. Tobushi K, Okumara M, Endo, Tanaka K (2002) Deformation behavior of TiNi shape memory alloy under strain- or stress-controlled conditions. Arch Mech 1(54):75–91.
11. Lin PH, Tobushi H, Tanaka K, et al. (1996) Influence of strain rate on deformation properties of TiNi shape memory alloy. JSME Int J A39(1):117–123.
12. Helm D, Haupt P (2001) Thermomechanical behavior of shape memory alloys, Proc. of SPIE's Smart Structures and Materials. SPIE 4333:302–313.
13. Shaw JA, Kyriakides S (1997) On the nucleation and propagation of phase transformation fronts in a TiNi Alloy. Acta Mater 45(2):683–700.
14. Shaw JA (2000) Simulation of localized thermo-mechanical behavior in NiTi shape memory alloy. Plasticity 16:541–562.
15. Gadaj SP, Nowacki WK, Tobushi H (1999) Temperature evolution during tensile test of TiNi shape memory alloy. Arch Mech 51(6):649–663.
16. Gadaj SP, Nowacki WK, Pieczyska EA (2002) Temperature evolution in deformed shape memory alloy. Infrared Physics & Tech 43:151–155.
17. Pieczyska EA, Gadaj SP, Nowacki WK (2002) Thermoelastic and thermoplastic effects investigated in steel, polyamide and shape memory alloys. Proc. of SPIE, Thermosense XXIV, Orlando, USA 4710:479–497.
18. Sun QP (2002) Phase transformation in superelastic NiTi polycrystalline micro-tubes under tension and torsion—from localization to homogeneous deformation. Int J Solids Struct 39:3797–3809.
19. Li ZQ, Sun QP (2002) The initiation and growth of macroscopic martensite band in nano-grained NiTi microtube under tension. Int J Plast 18:1481–1498.
20. He YJ, Sun QP (2005) Modeling and simulation of deformation pattern evolution during stress-induced martensite phase transformation in TiNi microtubes, TMS minerals. Metals & Materials Society.
21. Pieczyska EA, Gadaj SP, Nowacki WK, Tobushi H (2004) Investigation of nucleation and propagation of phase transitions in TiNi SMA. QIRT Journal 1(1):117–128.
22. Pieczyska EA, Gadaj SP, Nowacki WK, Tobushi H (2004) Thermomechanical investigations of martensite and reverse transformations in TiNi shape memory alloy. Bull Pol Ac: Tech 52-3:165–171.
23. Pieczyska EA, Gadaj SP, Nowacki WK, Tobushi H (2005) Transformation induced stress relaxation during superelastic behavior of TiNi SMA. Int J Appl Electromagn Mech 21:1–6.
24. Pieczyska EA, Gadaj SP, Nowacki WK, Tobushi H (2005) Phase-transformation front development and transformation-induced stress relaxation effects in TiNi shape memory alloy. Proc. 6th Internat. Conf. ICIM705, Tokyo:163–166.
25. Pieczyska E, Gadaj S, Nowacki WK, Hoshio K, Makino Y, Tobushi H (2005) Characteristics of energy storage and dissipation in TiNi shape memory alloy. Sci Technol Adv Mater 6:889–894.
26. Iadicola MA, Show JA (2004) Rate and thermal sensitivities of unstable transformation behavior in a shape memory alloy. Int J Plast 20-4/5:577–605.
27. Murasawa G, Koushinbou M, Yoneyama S, Sakuma T, Takashi M (2004) J Soc Mat Sci, Japan 53-9:999–1005.
28. Louche H, Chrysochoos A (2001) Thermal and dissipated effects accompanying Lüders band propagation. Mat Sci Eng A 307-1/2:15–22.
29. Sitner P, Liu Y, Novak V (2005) On the origin of Lüders like deformation of TiNi shape memory alloys. J Mech Phys Solids 53-8:1719–1746.
30. Matsui R, Tobushi H, Ikawa T (2004) Transformation-induced creep and stress relaxation of TiNi shape memory alloy. Proc Inst Mech Eng, J Materials: Design and Applications 218 Part L:343–353.